Granular Matter 5, 71–74 © Springer-Verlag 2003
DOI 10.1007/s10035-003-0127-9

A texture tensor to quantify deformations: the example of two-dimensional flowing foams

Marius Asipauskas, Miguel Aubouy, James A. Glazier, François Graner, Yi Jiang

Abstract In a continuum description of materials, the stress tensor field $\overline{\overline{\sigma}}$ quantifies the internal forces the neighbouring regions exert on a region of the material. The classical theory of elastic solids assumes that $\overline{\overline{\sigma}}$ determines the strain, while hydrodynamics assumes that $\overline{\overline{\sigma}}$ determines the strain rate. To extend both successful theories to more general materials, which display both elastic and fluid properties, we recently introduced a descriptor generalizing the classical strain to include plastic deformations: the "statistical strain," based on averages of microscopic details ("A texture tensor to quantify deformations" M.Au., Y.J., J.A.G., F.G, companion paper, *Granular Matter*, this issue). Here, we apply such a statistical analysis to a two-dimensional foam steadily flowing through a constriction, a problem beyond reach of both traditional theories, and prove that the foam has the elastic properties of a (linear and isotropic) continuous medium.

Received: 1 November 2002

M. Asipauskas
Dept. of Physics, 316 Nieuwland, University of Notre Dame, Notre-Dame, IN 46556-5670, USA

J. A. Glazier
Indiana Univerisity, Department of Physics,
Swain West 159, 727 East Third Street,
Bloomington, IN 47405-7105, USA

M. Aubouy
SI3M*, D.R.F.M.C., CEA, 38054 Grenoble Cedex 9 France
*U.M.R. n° 5819: CEA, CNRS and Univ. Joseph-Fourier

F. Graner
Laboratoire de Spectrométrie Physique**, BP 87,
38402 St Martin d'Hères Cedex, France
**U.M.R. n° 5588 : CNRS and Univ. Joseph-Fourier
Address for correspondence: graner@ujf-grenoble.fr
Fax: (+33) 4 76 63 54 95, BP 87, 38402

Y. Jiang
Theoretical Division, Los Alamos National Laboratory,
New Mexico 87545, USA

Thanks are due to S. Courty, B. Dollet, F. Elias, E. Janiaud for discussions. YJ is supported by the US DOE under contract W-7405-ENG-36. JAG acknowledges support from NSF, DOE and NASA contracts NSF-DMR-0089162, DOE-DE-FG0299ER45785 and NASA-NAG3-2366. We thank S. Cox for access to unpublished simulations.

Keywords Dispersed material, Foam, Stress-strain relation, Shear modulus

A "plastic" deformation means that microscopic rearrangements take place in the material, so that the microscopic pattern does not return to its initial condition even after the applied force has ended. An example of a highly heterogeneous one in a viscoelastic material is a two-dimensional foam steadily flowing through a constriction (Fig. 1). This apparently simple example is utterly intractable from the perspective of both elasticity theory [1] and Navier-Stokes [2] treatments. In this paper, we present a new approach to analyse complex flows of disordered materials.

We prepare the foam by blowing air into the bottom of a column of soap solution. The solution is 10% commercial dishwashing detergent ("Ivory" brand) and 5% glycerol. Its surface tension, measured by the Noüy method, is $\gamma = 28.5 \pm 0.1$ mN.m^{-1}. Filtered air blows at a steady flow rate of 0.08 cm^3.s^{-1} through an 18-gauge (0.084 cm ID) stainless steel needle with a 90° bevel. Bubbles are homogeneous in size (<5% dispersity), and float to the top of the column in random positions. The foam is dry, with a relative fraction of fluid <3%. Since a bubble edge (a film of soap solution) has two interfaces with air, its line tension λ is $\lambda = 2\gamma h = 28.5\ \mu$N.

Bubbles enter a horizontal channel, a Hele-Shaw cell made of two parallel Plexiglas plates $h = 0.5$ mm apart,

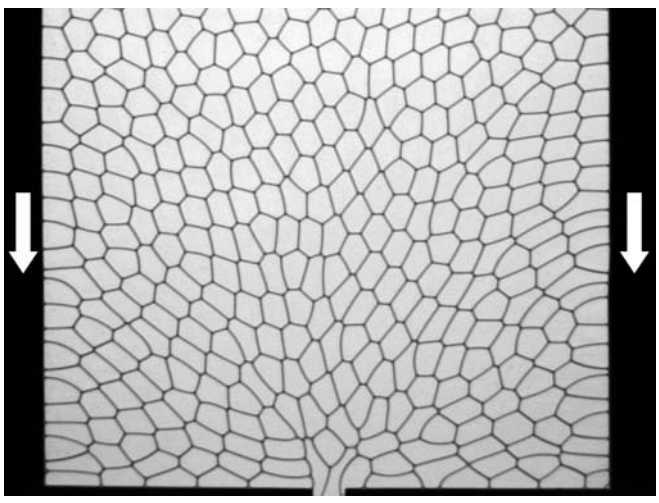

Fig. 1. Two-dimensional foam flowing through a constriction. The 10 cm (551 pixel) wide field of view shows only the end of the 1 m long horizontal channel

1 m long, and 10 cm wide (Fig. 1). The average bubble velocity is 0.1 cm.s^{-1}. The generation of new bubbles forces the mass of bubbles down the channel, in plug flow (free slip boundary conditions) if the channel were uniform. A 5-mm wide constriction near the end of the channel forces the flow to be heterogeneous. Beyond the constriction the bubbles reexpand into the full width channel for a short distance and then fall from the open channel end (no stress boundary conditions) into a collection vessel. The volume variations during the transit time (50 s) across the field of view, due to pressure differences or diffusion of gas from one bubble to its neighbours, are below our pixel induced detection limit of 2%.

All measurements we present use 60×60 pixel sliding boxes ("representative volumes"), meaning that we do not evaluate them within 30 pixels of the channel walls; and average over 2800 successive images of a 30 Hz movie. To measure the "Eulerian" velocity field, we track the center of mass of each bubble between two successive images and add the velocities of all bubbles in the same volume. The velocity field is smooth and regular (Fig. 2), qualitatively indicating that the foam behaves as a continuous medium.

To obtain a more quantitative characterization, we measure the stress in the foam. Stress has dissipative and elastic components; the pressure inside the bubbles and the network of bubble edges contribute to the latter. Since the pressure stress is isotropic, it does not contribute to the elastic normal stress difference $\overline{\overline{\sigma}}_{xx} - \overline{\overline{\sigma}}_{yy}$ (as measured for granular materials [3]) or the shear stress $\overline{\overline{\sigma}}_{xy}$, entirely due to the network. Dimensionally, $\overline{\overline{\sigma}}$ is of the order as the line tension λ (which, in a 2D foam, is the same for all edges: here 28.5 μN) divided by a typical bubble size.

We measure locally the network stress in each "representative volume element," that is, a square box, centered around the point of measurement, of a mesoscopic size: larger than a bubble, but much smaller than the channel width. We proceed as follows. We identify the bubble edges which cross the boundaries of the volume [4]. We determine the tension $\vec{\tau} = \lambda \hat{e}$ of each edge, where $\hat{e}$ is the unit vector tangent to the edge. We determine the average force $\vec{f}$ on a boundary element $d\vec{S}$ by vectorially adding these tensions and obtain $\overline{\overline{\sigma}}$ defined by: $f_i = \overline{\overline{\sigma}}_{ij} dS_j$ [1, 5]; equivalently, we may use an average over all links to improve the statistics [6,7].

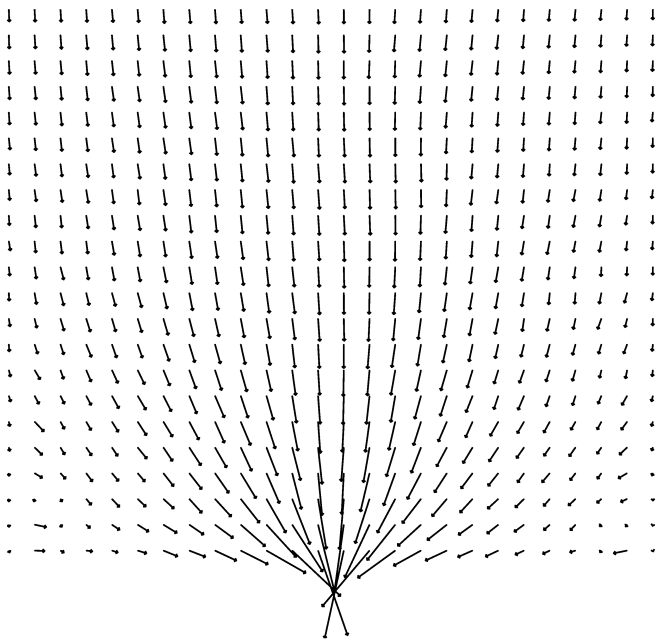

Fig. 2. Velocity field in the foam (in arbitrary units, the same scale for each arrow)

Clearly, the stress field is strongly heterogeneous (Fig. 3). The upstream influence of the constriction becomes visible as the lobe where $\overline{\overline{\sigma}}_{xx} - \overline{\overline{\sigma}}_{yy}$ changes sign.

To characterize the deformation of the bubbles, we consider a volume $\mathcal{V}(\vec{R})$ around the position $\vec{R}$. In this volume, we list all pairs $(\vec{r}, \vec{r}')$ of positions of neighboring vertices connected by one bubble edge. From the vector $\vec{\ell} = \vec{r}' - \vec{r}$, we construct the tensor $\vec{\ell} \otimes \vec{\ell} = (\ell_i \ell_j)$. This tensor averaged over $\mathcal{V}(\vec{R})$ defines the local "texture tensor" $\overline{\overline{M}}(\vec{R})$:

$$M_{ij} = \langle \ell_i \ell_j \rangle_{\mathcal{V}(\vec{R})},$$

see details in the companion paper [7]. This symmetric tensor has two strictly positive eigenvalues, both of order $\langle \ell^2 \rangle$, the largest being in the direction in which bubbles elongate. It reflects at large scales the relevant features of the actual microstructure of the material. For instance, Fig. 4 shows an example of $\overline{\overline{M}}(\vec{R})$ measured in the flowing foam experiment of Fig. 3. This texture tensor $\overline{\overline{M}}(\vec{R})$ thus quantifies the qualitative impression of compression or elongation we obtain by looking at the bubbles in each region of Fig. 1. The smooth and continuous variations of the statistical strain tensor field in space validate treating the foam as a continuous medium.

We have defined the "statistical strain tensor" [7]:

$$\overline{\overline{U}}(\vec{R}) = \frac{1}{2} \left(\log \overline{\overline{M}}(\vec{R}) - \log \overline{\overline{M}}_0 \right).$$

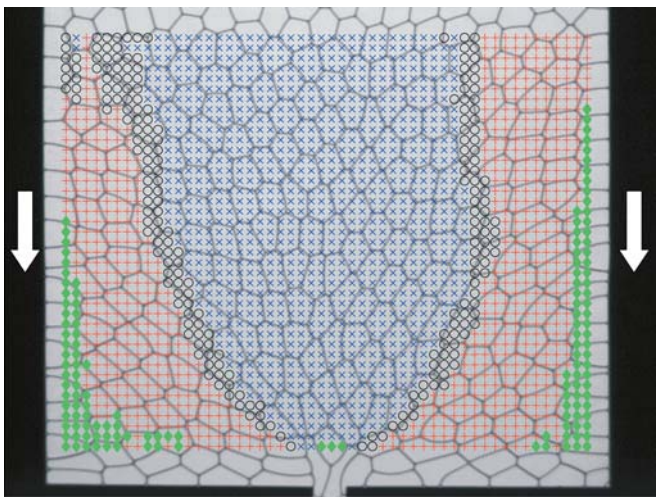

Fig. 3. Snapshot of the foam (Fig. 1) with regions colored according to the sign of the experimental value of the normal elastic stress difference $\overline{\overline{\sigma}}_{xx} - \overline{\overline{\sigma}}_{yy}$: blue $\times$, negative; black $\circ$, zero within error; red $+$, positive; green $\diamond$, values we omit in Fig. 5

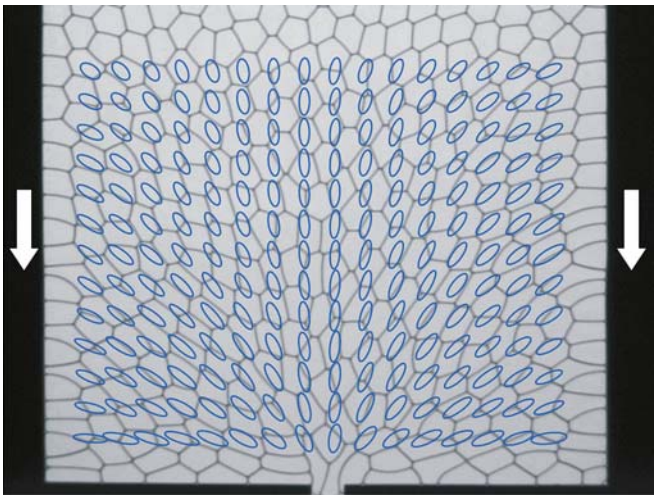

Fig. 4. Experimental measurement of $\overline{\overline{M}}(\vec{R})$, superimposed on a snapshot of the foam (Fig. 1). Since $\overline{\overline{M}}$ is a real symmetric tensor with strictly positive eigenvalues, we display it as an ellipse, the length of each axis (in arbitrary units, the same scale for each ellipse) being proportional to an eigenvalue. We omit data on boxes touching the channel wall

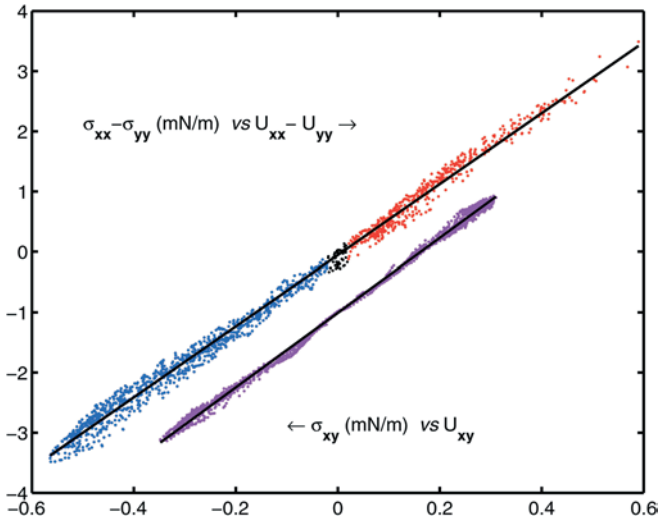

Fig. 5. Plot of $\overline{\overline{U}}$ versus $\overline{\overline{\sigma}}$. The color code is the same as in Fig. 3, showing the sign of the normal stress difference $\overline{\overline{\sigma}}_{xx} - \overline{\overline{\sigma}}_{yy}$: blue, negative; black, zero within error bars; red, positive. We omit data from the boxes touching the channel wall. The black line is a linear fit. On the same graph, we plot $\overline{\overline{\sigma}}_{xy}$ (violet) *vs* $\overline{\overline{U}}_{xy}$, shifted by -1 mN.m^{-1} for clarity

Here the reference value $\overline{\overline{M}}_0$ is chosen in the undeformed, isotropic foam far upstream of the constriction (a choice that plays no role in elastic properties): $\overline{\overline{M}}_0 = \langle \ell_0^2 \rangle \overline{\overline{I}}/2$, where $\overline{\overline{I}}$ is the identity tensor, here in two dimensions. By definition, we calculate the tensor $\log \overline{\overline{M}}$ by rotating $\overline{\overline{M}}$ to a basis where it is diagonal, taking the logarithm of its eigenvalues, then rotating it back into the initial basis (this definition is more convenient than the equivalent one using a development as an infinite series). Hence $\log \overline{\overline{M}}$ has the same axes as $\overline{\overline{M}}$, and is real and symmetric.

The "statistical strain" tensor $\overline{\overline{U}}$ reduces to the usual definition of strain $\overline{\overline{u}}$ in the validity limits of classical elasticity [7]. It is purely geometric, and does not explicitly depend on stresses and forces. It applies to a whole general class of materials with both elasticity and plastic rearrangements, whether 2D or 3D, whenever we can experimentally measure the relevant information: whether detailed (list of microscopic positions and links) or mesoscopic averages (quantities related to $\overline{\overline{M}}$). It is a state variable, constant in a steady flow, and is not necessarily homogeneous through the whole sample, allowing a thermodynamic description of non-equilibrium complex fluids [8].

Do the elastic stress and the statistical strain relate deterministically? In Fig. 5 we plot the normal stress difference $\overline{\overline{\sigma}}_{xx} - \overline{\overline{\sigma}}_{yy}$ versus $\overline{\overline{U}}_{xx} - \overline{\overline{U}}_{yy}$; in this representation, the isotropic contributions (of $\overline{\overline{M}}_0$ in $\overline{\overline{U}}$, and of the pressure stress in $\overline{\overline{\sigma}}$) play no role, hence we refer only to the foam's current state. Each data point is a measurement which derives from averages at one position of the foam: data sources are the same as in Figs. 3 and 4. That is, in principle Fig. 5 measures a constitutive relation from a single image; in practice, we average 2800 similar images to improve the precision.

Since $\overline{\overline{M}}$, and hence $\overline{\overline{U}}$, is completely independent of $\overline{\overline{\sigma}}$ [7], the high correlation between $\overline{\overline{U}}$ and $\overline{\overline{\sigma}}$ apparent in Fig. 5 reflects the physical constitutive relation required to treat the foam as a continuous medium, in which details of the microstructure appear only through mesoscopic averages. Since different applied strains $\overline{\overline{u}}_{appl}$ can correspond to the same $\overline{\overline{\sigma}}$, such a relation does not appear in classical $\overline{\overline{\sigma}}$ *vs.* $\overline{\overline{u}}_{appl}$ plots [6].

Moreover, the relation between $\overline{\overline{U}}$ and $\overline{\overline{\sigma}}$ is linear over the whole range covered by this experiment. The slope of Fig. 5 measures 2μ, where μ is the shear modulus of the foam, much beyond the validity regime of classical elasticity. We find, for the $xx - yy$ component:

$$\mu_{xx-yy} = 3.00 \pm 0.005 \text{ mN.m}^{-1}.$$

The foam is nearly isotropic, since we find almost the same value for the xy component:

$$\mu_{xy} = 3.06 \pm 0.01 \text{ mN.m}^{-1}.$$

Note that we find similar values, 3.00 ± 0.01 mN.m^{-1} and 3.01 ± 0.01 mN.m^{-1} respectively, for a foam flowing relatively to a fixed round obstacle (data not shown). A regular "honeycomb" hexagonal lattice has an isotropic shear modulus $\mu_h = \lambda/(\ell\sqrt{3})$, hence with the same tension and average bubble area $\langle A \rangle$ it would have a shear modulus $\mu_h = 0.465\ \lambda/\sqrt{\langle A \rangle} = 2.52$ mN.m^{-1} [9–11]. Our value $\mu = 3.0$ is higher: $\mu/\mu_h = 1.2$. This difference is likely due to the side length disorder $\langle \ell^2 \rangle / \langle \ell \rangle^2 = 1.22$ of the foam. How μ/μ_h depends on the microstructure and its disorder is an open problem [12].

We have performed the following tests of the validity of our method. We have checked the agreement between our measurement of statistical strain and the classical strain, first analytically on a honeycomb lattice, then numerically on a disordered simulated foam kept in the elastic regime

[13]. We have checked that if we increase the size of the volume element, we decrease the fluctuations, and thus the upper and lower values of $\overline{\overline{\sigma}}$ and $\overline{\overline{U}}$ in Fig. 5, but the slope and hence μ are unchanged. Finally, the value of the shear stress tensor field or shear modulus, resulting from our image analysis, predicts the force exerted by the flowing foam on an obstacle. We have tested it against an independent, macroscopic measurement of the force, and found that they agree (S. Courty *et al.*, in preparation).

In summary, we have measured the stress, the texture tensor and the statistical strain for a 2D flowing foam. We have shown that the 2D foam behaves like a linear and isotropic continuous material.

References

1. L. D. Landau & E. M. Lifschitz, Theory of Elasticity (Reed Educational and Professional Publishing, Oxford, 3rd edition 1986)
2. L. D. Landau & E. M. Lifschitz, Fluid Mechanics (Reed Educational and Professional Publishing, Oxford, 2nd edition 2000)
3. A. Meheboob & S. Luding, Rheology of bidisperse granular mixtures via event driven simulations (2002), to appear in J. Fluid Mech.
4. In practice, we approximate $\hat{e}$ by using the unit vector of the chord connecting the two vertices. This is correct for a 2D foam at equilibrium [F. Graner, Y. Jiang, E. Janiaud, C. Flament, Phys. Rev. E 63 (2001) pp. 011402/1-13]. In a 2D foam at low flow rate, the error we introduce is negligible
5. L. E. Malvern, Introduction to the Mechanics of a Continuous Medium (Prentice-Hall, Inc., New Jersey, 1969)
6. D. A. Reinelt & A. M. Kraynik, J. Rheol. 44 (2000), p. 453
7. M. Aubouy, Y. Jiang, J. A. Glazier, & F. Graner, A texture tensor to quantify deformations. Companion paper, Granular Matter, 5 (2003), pp. 67–70
8. G. Porte, J.-F. Berret & J. Harden, J. Phys. II France 7 (1997), p. 459
9. D. Weaire & S. Hutzler, *Physics of Foams* (Oxford Univ. Press, Oxford, 1999)
10. H. M. Princen, *J. Coll. Interf. Sci.* 91 (1983), p. 160
11. S. Khan & R. Armstrong, J. Non-Newtonian Fluid Mech 22 (1986), p. 1
12. S. Alexander, Phys. Reports 296 (1998), p. 65
13. S. Cox, private communication (2002)